Supplementary Figure Legends

Supplementary Fig. 1|Immune Cell Profiling by Multi-Color Flow Cytometry. **a**, common gating for viable CD45+ cells. **b**, Gating hierarchy for T cell lineage and phenotypic marker. **c**, Myeloid cell gating hierarchy. **d**, Gating for NK lineage and Tregs.

Supplementary Fig. 2|Immune Cell Profiling of MDOTS. **a-b**, Mean fluorescent intensity (MFI) of major leukocyte lineage markers (**a**) and lymphocyte and monocyte phenotypic markers (**b**) with and without exposure to collagenase (type IV) and DNase. **c,** comparison of gated populations +/- collagenase (type IV) and DNase I (R^2 = 0.991), as previously described (44). **d**, Immune cell sub-populations from MC38 bulk tumor (n=5) to S1, S2, S3 (n=6) were evaluated by flow cytometry, as in Fig. 1b (Kruskal-Wallis test with Dunn's multiple comparisons test, α=0.05; *p<.05; *ns*=not significant). **e**, Pearson correlation matrix using composite of 21 cell surface markers in MC38 tumor, S1, S2, and S3 spheroids (Table S1). **f**, CD45+ cells (%live cells) in MC38 (n=6), CT26 (n=5), and B16F10 (n=5) MDOTS (S2). Kruskal-Wallis test with Dunn's multiple comparisons test, α=0.05; *p<.05. **g**, immune sub-populations (%CD45+ cells) in MC38 (n=6), B16F10 (n=5), and CT26 (n=5) MDOTS (S2). 2-way ANOVA with Tukey's multiple comparisons test, α=0.05; *p<.05, ***p<.001, ****p<.0001). **h**, Immunohistochemical staining for CD45+ and CD8+ cells and quantitation of CD8+ cells in FFPE sections from an explanted MC38 tumor (average of 10 high power fields, 200x magnification). **i**, Spheroid size evaluation of MC38 MDOTS (Day 6) stained with AO/PI.

Supplementary Fig. 3|*In vivo* and *ex vivo* profiling of PD-1 blockade. a, Live/dead analysis of MC38 MDOTS ± anti-PD-1 performed by independent lab (n=3, biological replicates). **b,** Live/dead analysis of Lewis lung carcinoma (LLC) MDOTS ± anti-PD1 (n=2, biological replicates, *ns* = not significant). **c-d**, Live/dead analysis of MC38 MDOTS (c, Day 6) and GL261 MDOTS (d, Day 5)

following treatment with isotype IgG control (10 μg/mL) or anti-PD-1 (10 μg/mL) ± anti-CD8 (10 μg/mL) (n≥3, biological replicates; 2-way ANOVA with Tukey's multiple comparisons test; **p<.01, ***p<.001, ****p<.0001, *ns* = not significant). **e,** MC38 MDOTS stained for CD45+ immune cells (purple) and CD8+ T cells (yellow) with calcein (green) staining live cells and Hoechst (blue) staining all cell nuclei at Day 7 after treatment with IgG (10 μg/mL) or anti-PD-1 (10 μg/mL) (scale bar = 20 μm). Colors are virtually adjusted for better representation. **f,** Comparison of intra-tumoral and inter-tumoral heterogeneity evaluating CD8+ T cell counts (IF, performed on Day 4) and live/dead analysis (AO/PI staining) of CT26 MDOTS (Day 5) (n=3, biological replicates; 2-way ANOVA with Tukey's multiple comparisons test; ****p<.0001, *ns* = not significant).

Supplementary Fig. 4|Synthesis and evaluation of a novel TBK1/IKBKE inhibitor. a, Absolute cytokine levels in CT26 MDOTS over time (n=3, biological replicates). **b-c**, Live/Dead analysis at Day 6 (b) and heatmap of relative cytokine changes (c) in CT26 MDOTS treated with anti-CCL2 ± anti-PD-1 at Days 1, 3, and 6 (L2FC relative to isotype control; n=3, biological replicates). **d,** Chemical synthesis of Compound 1. **e**, IC_{50} curves for TBK1 and IKKε (IKBKE). **f,** Effect of Compound 1 on viability of CT26 spheroids lacking immune cells (n=3, biological replicates; 2-way ANOVA with Sidak's multiple comparisons test; *ns* = not significant). **g,** Percent-change in IL-2 levels produced by Jurkat cells with increasing doses of Compound 1. **h,** Re-implantation of CT26 and EMT-6 cells into the flanks of a mouse previously treated with anti-PD-L1+ Compound 1.

Supplementary Fig. 5|Immune Cell Profiling of PDOTS. **a-b**, Surface expression of T cell exhaustion markers (PD-1, CTLA-4, TIM-3) on (a) CD4 and (b) CD8 populations in PDOTS (n=40). **c**, Surface expression of PD-L1 and PD-L2 on myeloid sub-populations, including granulocytic myeloid-derived suppressor cells (gMDSCs), monocytes, tumor-associated macrophages (TAMs), monocytic myeloid-derived suppressor cells (mMDSCs), and plasmacytoid dendritic cells (pDCs). **d**, Immune cell

sub-populations of PDOTS fractions (S1, S2, S3) evaluated by flow cytometry, for CD45+ (n=8), CD3+ (n=8), CD4+ (n=7), CD8+ (n=7), CD14+ (n=7), and CD15+ (n=6). Kruskal-Wallis test with Dunn's multiple comparisons test, α=0.05; *ns*=not significant. **e-f**, Antigen-experienced sub-population (CD45RO+), effector memory (CD45RO+CCR7-) subtype, and surface expression of T cell exhaustion markers (PD-1, CTLA-4, TIM-3) on CD4 (e) and CD8 (f) populations in PDOTS fractions ($n \geq 3$; Kruskal-Wallis test with Dunn's multiple comparisons test, α=0.05; *ns*=not significant). **g-k**, Live/dead analysis (g) of PDOTS (early stage resected NSCLC tumor, Day 7) in response to αPD-1 (250 μg/mL pembrolizumab), αPD-L1 (600 μg/mL atezolizumab), or IFNγ (200 ng/mL), and baseline immune profiling (h-k) of PDOTS from the same NSCLC tumor, demonstrating percent CD45+ cells (h), percent lymphoid and myeloid subsets (i), percent CD4 and CD8 T cells (j), and CD4/CD8 T cell subsets (k), demonstrating abundance of effector memory CD4 and CD8 T cells.

Supplementary Fig. 6 | Cytokine Profiling of PDOTS. a-c, Absolute cytokine levels (pg/mL) obtained by bead-based cytokine profiling of PDOTS under control conditions or in response to αPD-1 grouped by (a) Th1 and IFN-γ effector cytokines, (b) granulocyte chemoattractants, and (c) IPRES immune suppressive cytokines, (n=28; 2-sided, paired, *t*-test, α= 0.05). **d,** Comparison of PDOTS cytokine profiles after 3 days in standard growth conditions with and without isotype control IgG antibody (50 μg/mL) (n=2). Performed using PDOTS derived from sample MGH-16 (melanoma). **e,** CCL19 and CXCL13 levels (pg/mL) relative to the number of spheroids per device in control and treatment (αPD-1) conditions (R^2 = Pearson correlation coefficient). **f-g,** Biological replicates for MGH-16 PDOTS in response to PD-1 blockade (n=3, L2FC relative to untreated control on Day 3). **h,** Correlation between CCL19 and CXCL13 upregulation (log2 fold-change relative to untreated control) in response to αPD-1, αCTLA-4, or αPD-1 + αCTLA-4 (R^2 = Pearson correlation coefficient). **i,** Effect of culture in the microfluidic device on cytokine profile following αPD-1 treatment. Equal volumes of PDOTS from patient MGH-16 (in collagen hydrogels) were loaded for microfluidic device (or into a single well of a 96-

well plate in equal volumes of culture media. Media was collected on Day 3 (control and αPD-1) for cytokine profiling. Induction of cytokines represented as fold-change relative to the untreated control.

Supplementary Fig. 7|Single and Dual Immune Checkpoint Blockade in PDOTS. a-d, Heatmaps demonstrating log(2) fold-change (relative to untreated control, ranked highest to lowest) in cytokine profiles using conditioned media obtained at indicated time points of *ex vivo* microfluidic culture with αPD-1, αCTLA-4, or αPD-1 + αCTLA-4. Arrows denote effector cytokines (e.g. IFN-γ, IL-2) associated with immune-mediated cytolysis. **a**, DFCI-25 (melanoma PDOTS). **b**, MGH-12 (melanoma PDOTS). **c**, DFCI-16 (thyroid carcinoma PDOTS). **d**, DFCI-19 (pancreatic adenocarcinoma PDOTS).

Supplementary Fig 8| Cellular and Tissue Sources of CCL19 and CXCL13. a, PDOTS were divided into CCL19/CXCL13-high (n=14) and CCL19/CXCL13-low (n=14) by median L2FC (Mann-Whitney test, ****p<.0001). **b,** Median immune cell composition (CD45+, CD4+, CD8+, CD14+, CD15+) between PDOTS with distinct ex vivo expression of CCL19/CXCL13 (high vs. low). **c,** Median immune cell composition (CD4+PD1+ and CD8+PD-1+) in CCL19/CXCL13 high vs. low PDOTS. **d,** Relative expression of CCL19 and CXCL13 by qRT-PCR in cancer-associated fibroblasts (CD45-CD90+), cancer-associated endothelial cells (CD31+CD144+), CD45- (cancer cells, etc.) and CD45+ immune cells following 4-way cell sorting (n=2, technical replicates from MGH-16). **e,** immunohistochemical staining of CCL19, CXCL13, αSMA (cancer-associated fibroblasts), and CD31 (endothelial cells) in melanoma specimen (pt 422, on-treatment; 40x magnification, scale bar 400 μm). **f,** CCL19 and CXCL13 levels in MC38 MDOTS treated with IgG isotype control (10 μg/mL), αPD-1 (10 μg/mL), αPD-1 + αCD8 (10 μg/mL, each), or IFNγ (200 ng/mL) at Days 1, 3, 6 of *ex vivo* culture. **g,** CCL19 levels in lysates from a CT26 tumor and a tumor-draining lymph node (lymph node) obtained from a mouse with prolonged response to PD-1 blockade (treated biweekly with αPD-1 for 3 weeks, starting at Day 8; tumor and tumor-draining lymph node collected on Day 70 following implantation).

Supplementary Fig. 9| Evaluation of CCL19, CXCL13, and Candidate Effector Molecules in Melanoma. a, RNA-seq showing select cytokines, cytokine receptors, cytotoxic T cell (CTL) associated genes, and IPRES transcripts (L2FC relative to pre-treatment control) in indicated sets of patient samples (group A - immune infiltrated; group B – immune poor by ssGSEA, Fig. 7c). **b-c**, RNA-seq absolute expression (RPKM) for (b) cytotoxic T cell effector associated genes (IFNG, IFNGR1, granzyme A, granzyme B) and (c) select IPRES genes in melanoma biopsy specimens (pre- and on-treatment) from group A (n=10 samples from 4 patients) or group B (n=17 samples from 6 patients). **d,** Box and whisker plots of OS and PFS using RNA-seq patient samples (Mann-Whitney test; **p<.01, *ns* = not significant). **e**, Kaplan-Meier survival curve by (f) CCL19/CXCL13 expression (high vs. low) using cutaneous melanoma (SKCM) TCGA data (38) (log-rank Mantel-Cox test; ***p<.001).

Supplementary Fig 10|Cytokine profiles and response to PD-1 blockade. a, Patients (from PDOTS and RNA-seq studies were stratified into response groups based duration of overall survival (OS) and duration of progression-free survival (PFS). Clinical benefit (CB) was defined as OS >360 days and PFS >180 days (n=9). No clinical benefit (NCB) was defined as OS <360 days (n=6). An additional cohort of patients who achieved long-term survival (OS > 360 days) with early tumor progression (PFS <180 days; n=9). **b-c,** Box and whisker plots of PFS (b) and OS (c) using PDOTS and RNA-seq patient samples grouped by response (Kruskal-Wallis with Dunn's multiple comparisons test; *p<.05, **p<.01, ***p<.001). **d,** Composite IPRES (14) score (sum of L2FC for CCL2, CCL7, CCL8, CCL13, IL-10) in response to *ex vivo* PD-1 blockade in PDOTS samples grouped by response. **e**, Heatmaps of Day 3 PDOTS anti-PD1 induced cytokines for samples DFCI-13, -16, -18, and -21 (serial sampling from same patient with metastatic papillary thyroid cancer), expressed as L2FC relative to untreated control. **f**, Serial immune profiling of samples DFCI-13, -16, -18, -21, and -22 from the same patient undergoing indicated treatments.

Supplementary Fig. 1

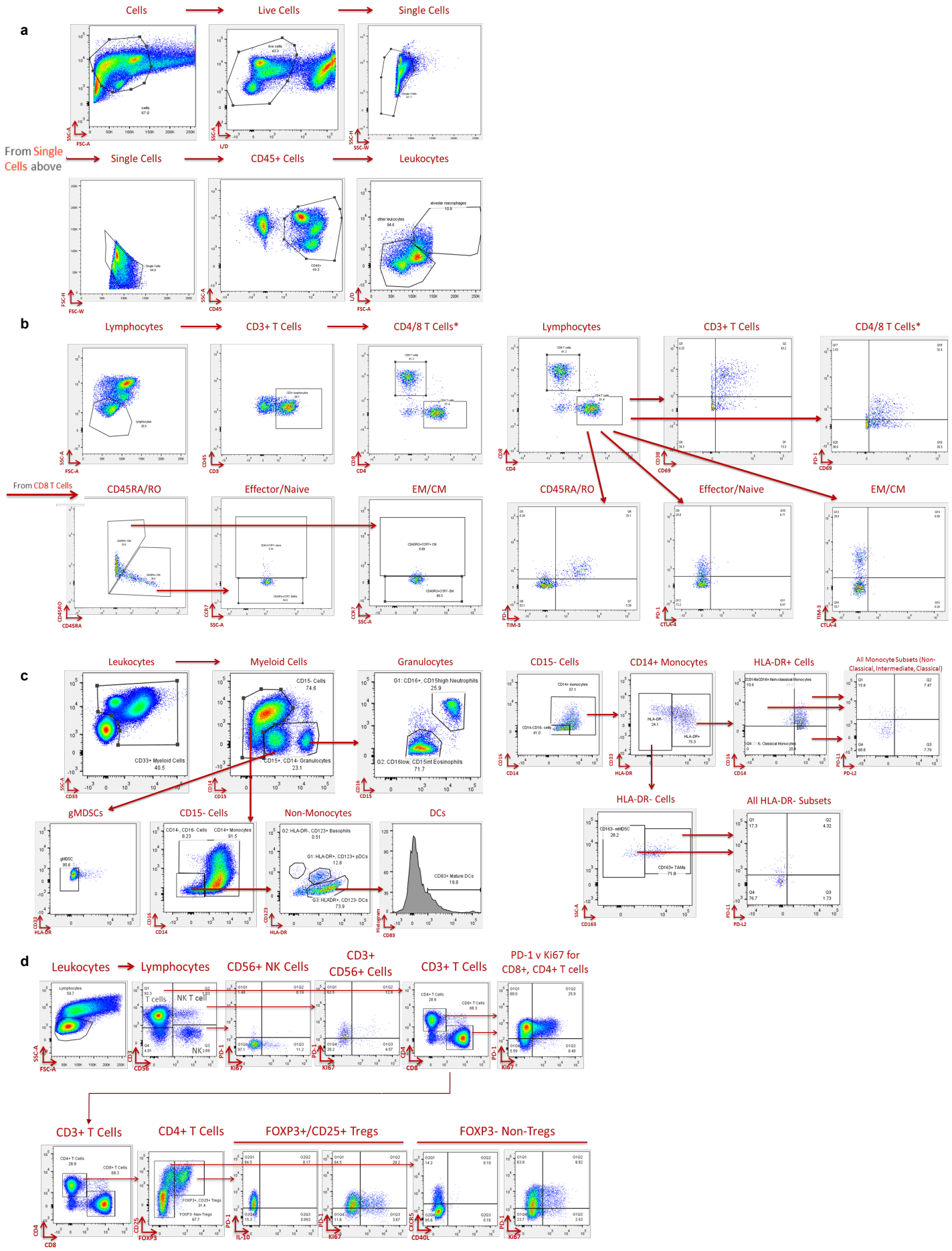

Supplementary Fig. 2

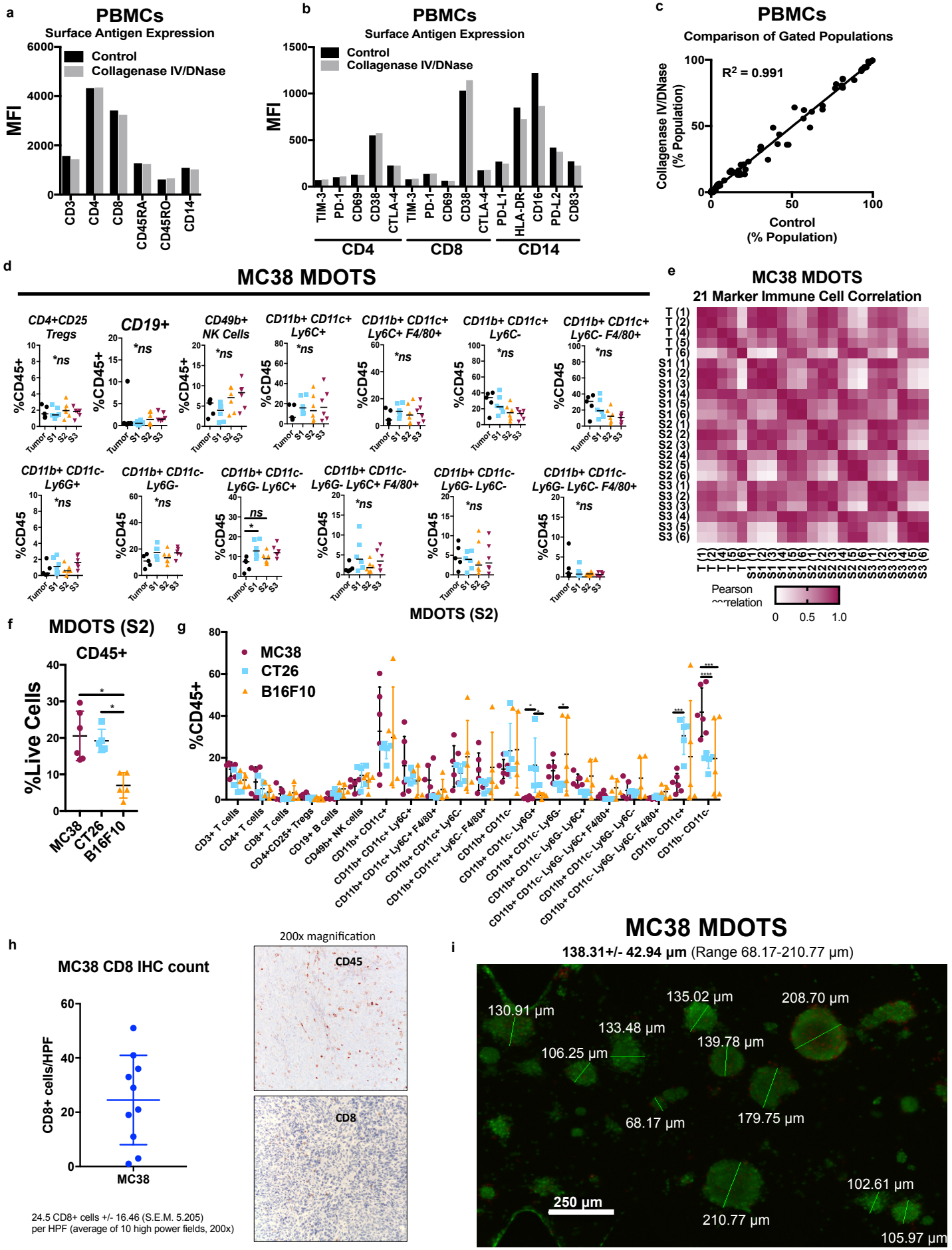

Supplementary Fig. 3

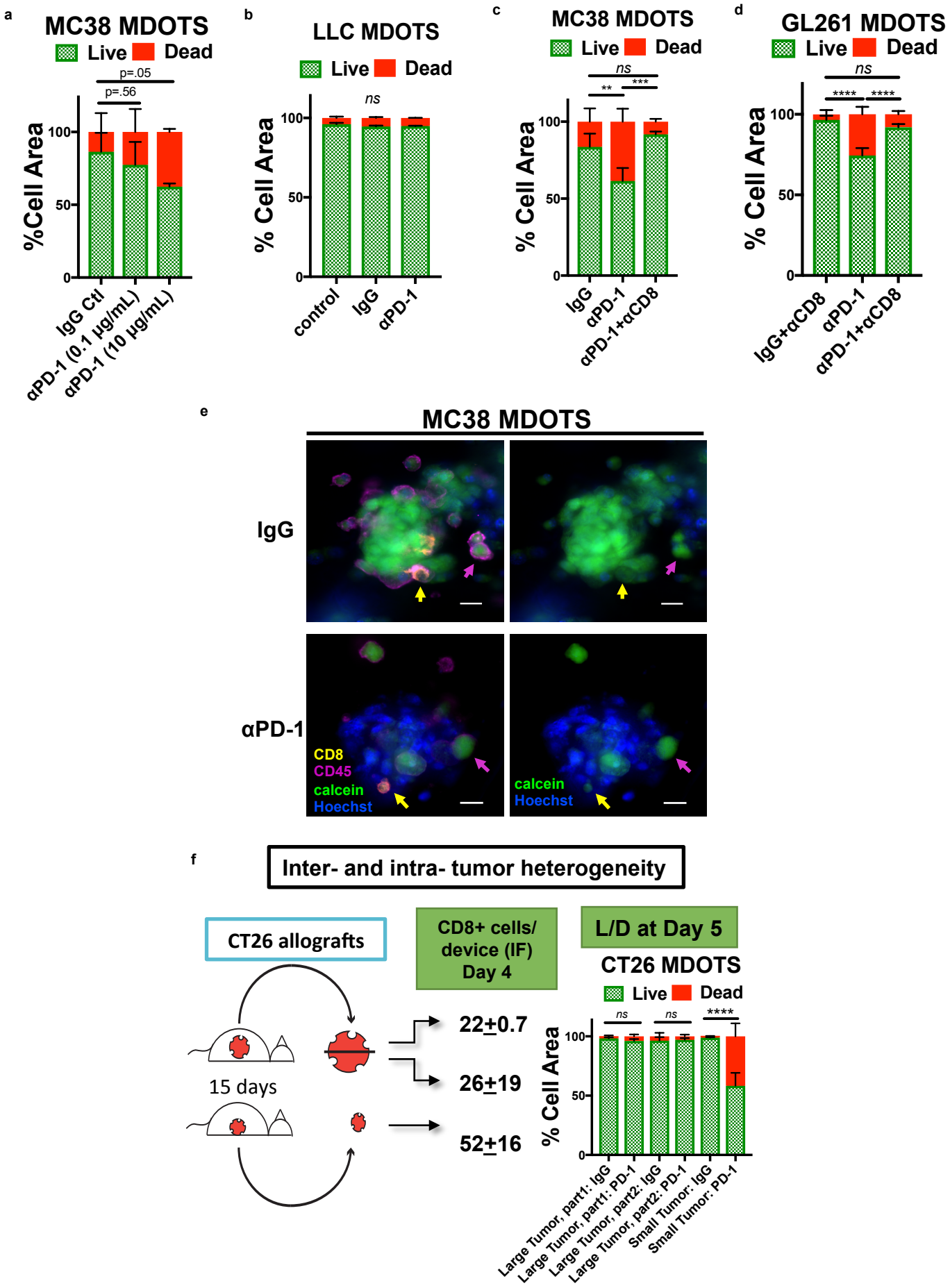

Supplementary Fig. 4

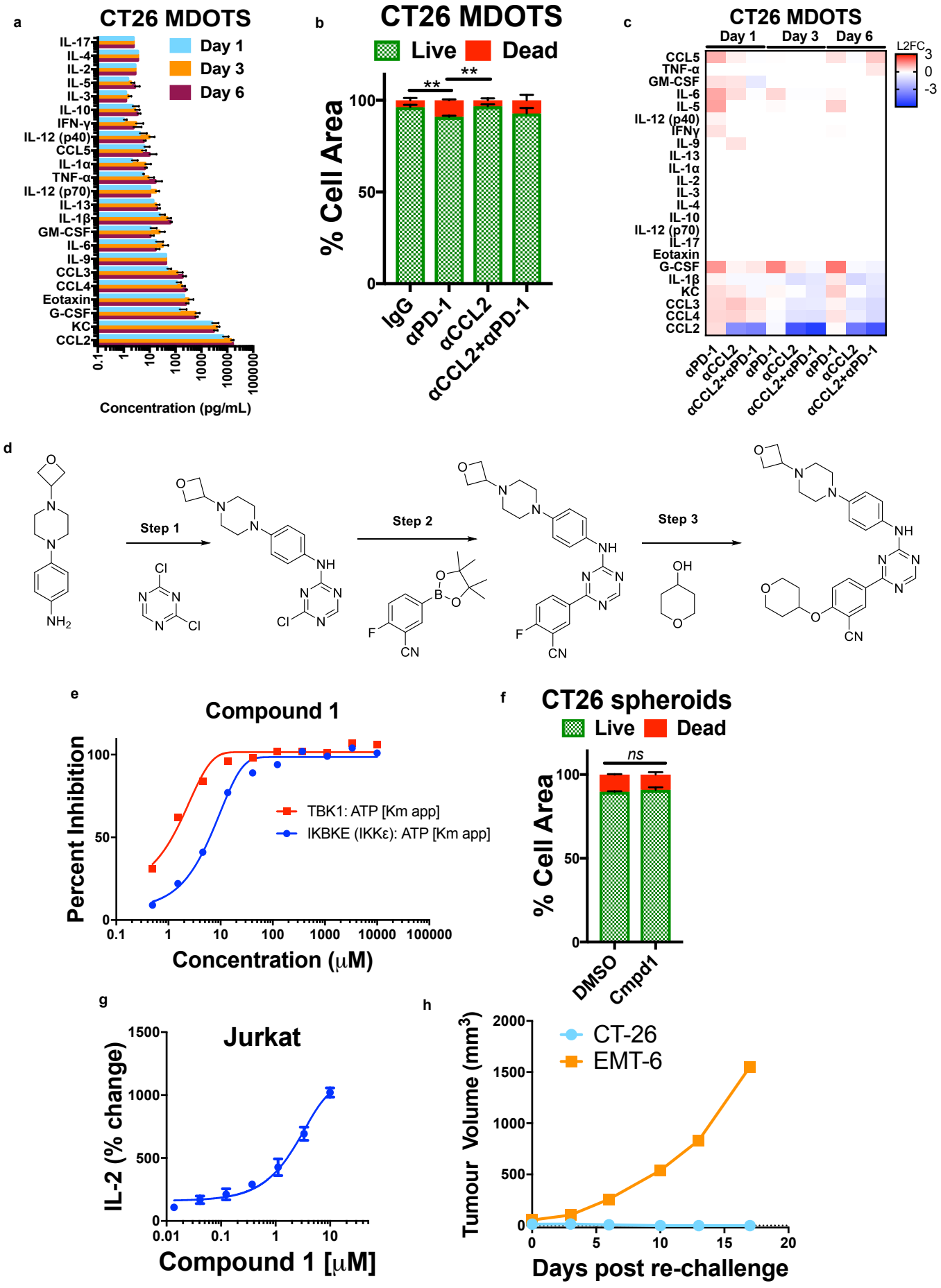

Supplementary Fig. 5

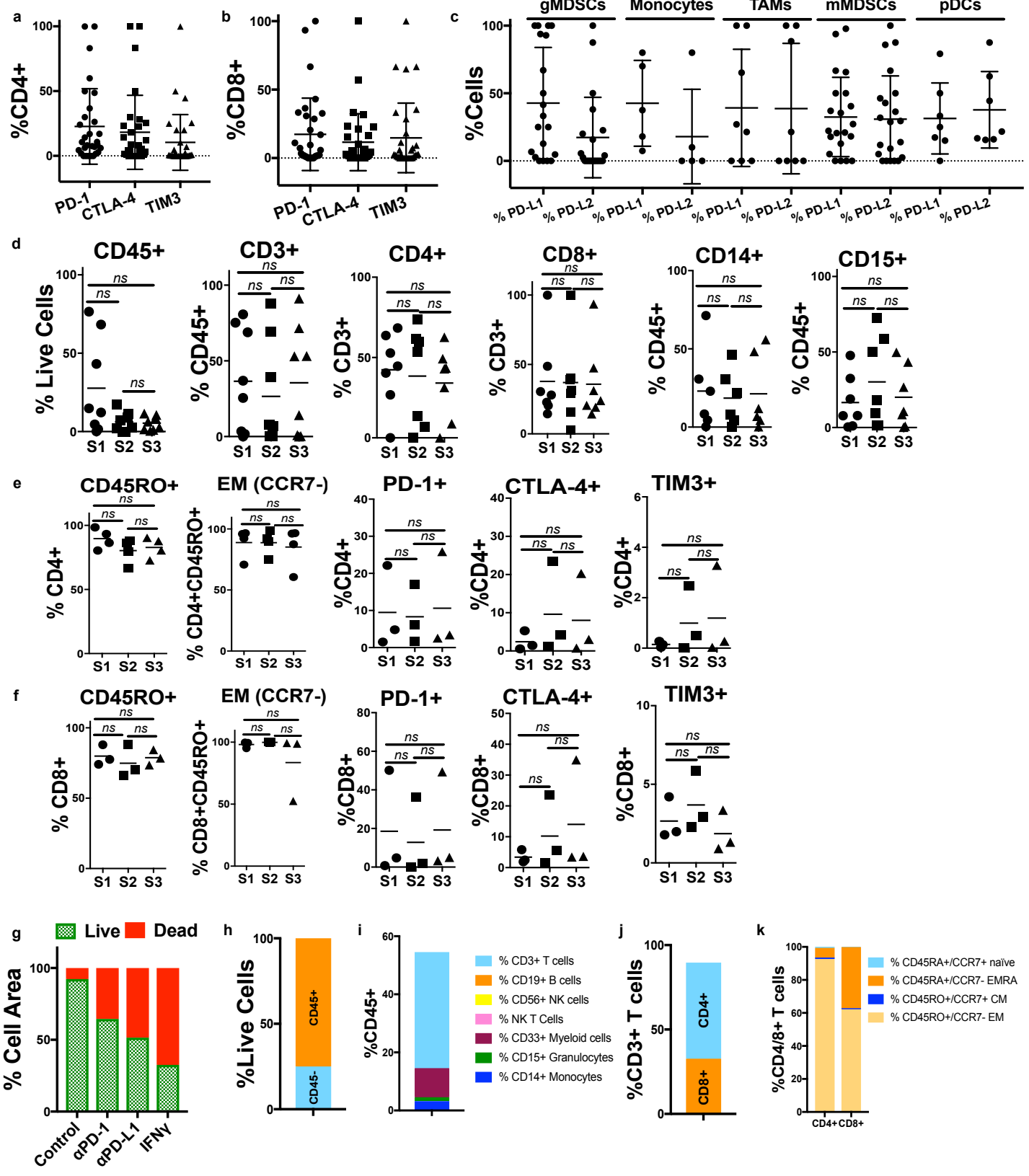

Supplementary Fig. 6

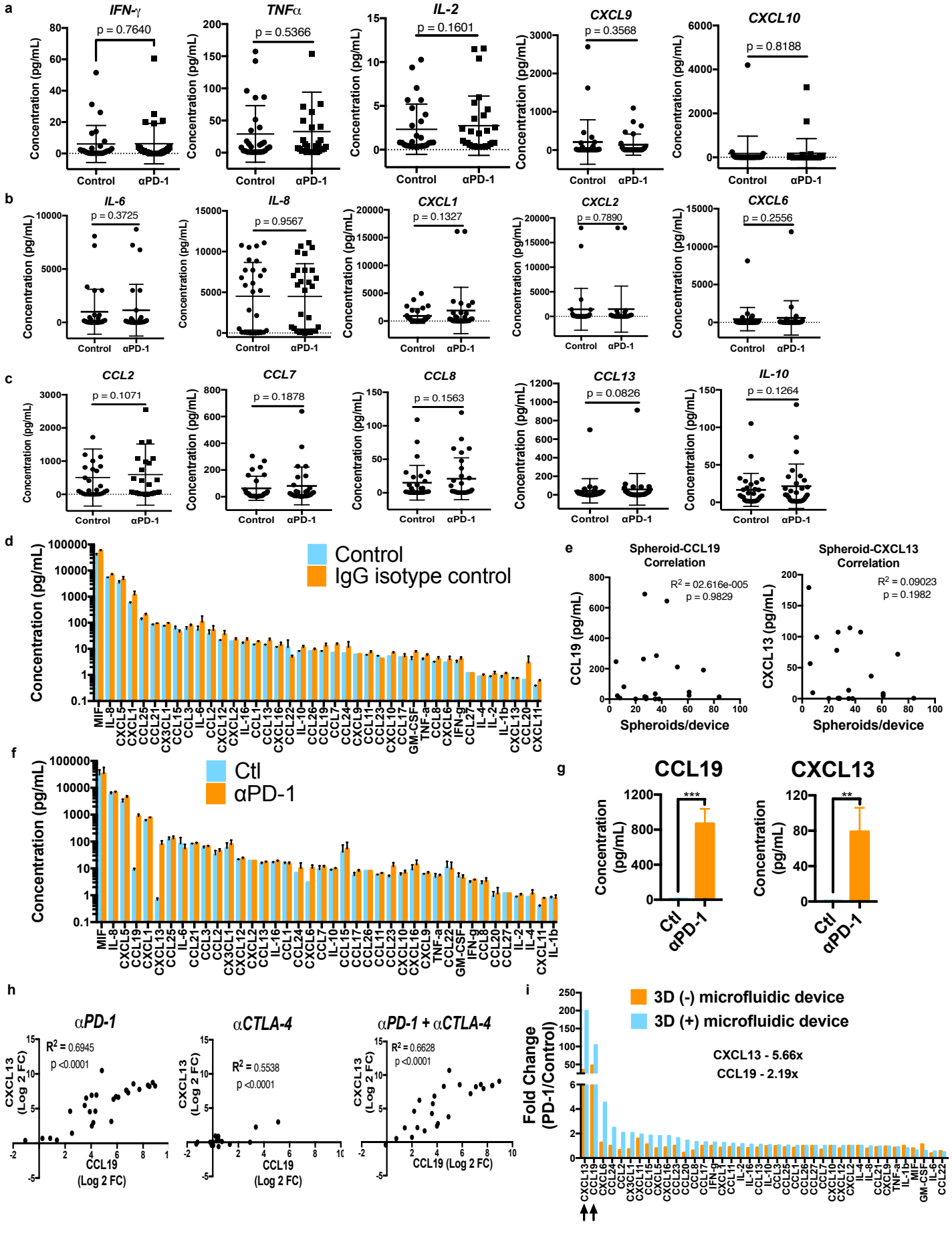

Supplementary Fig. 7

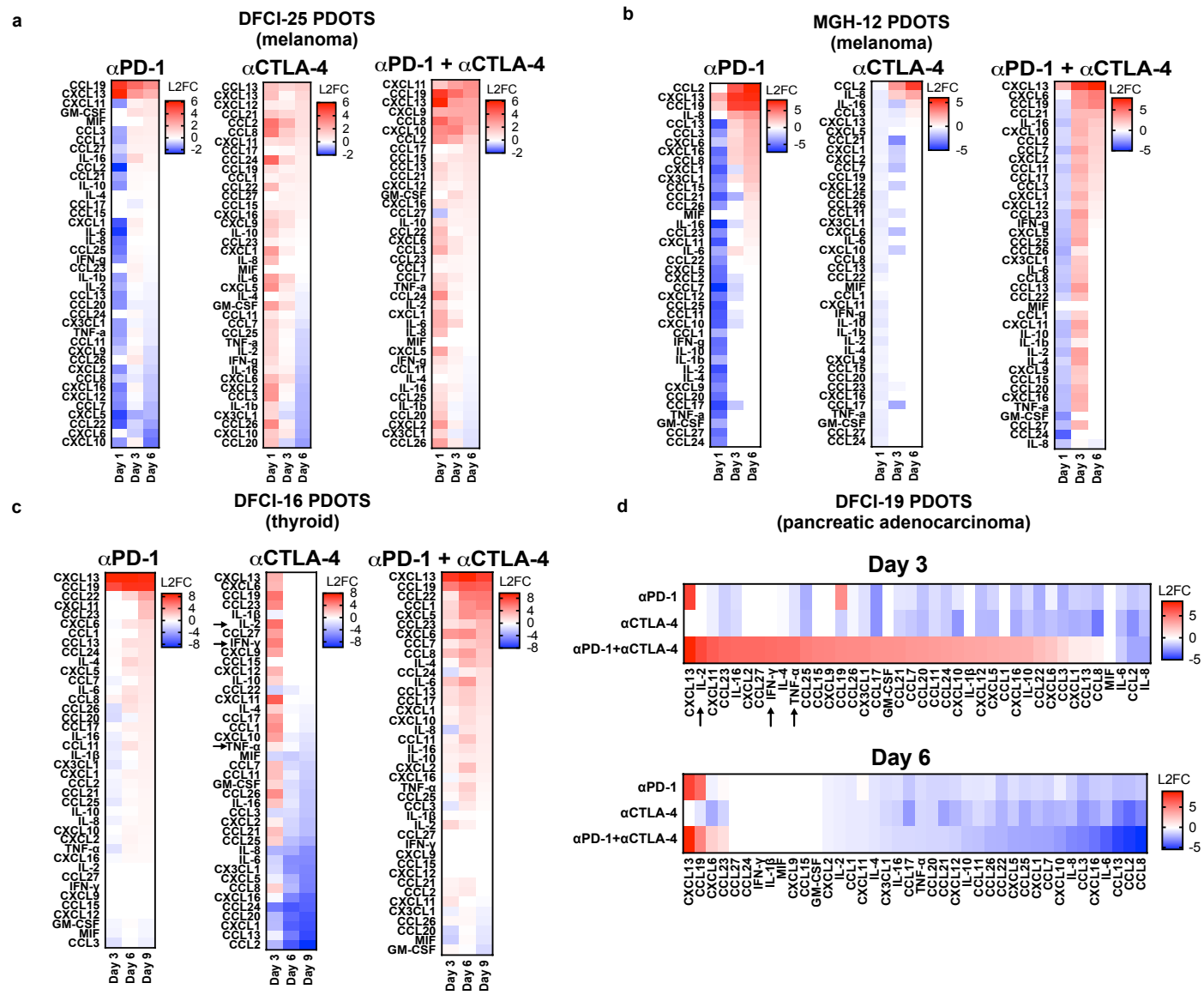

Supplementary Fig. 8

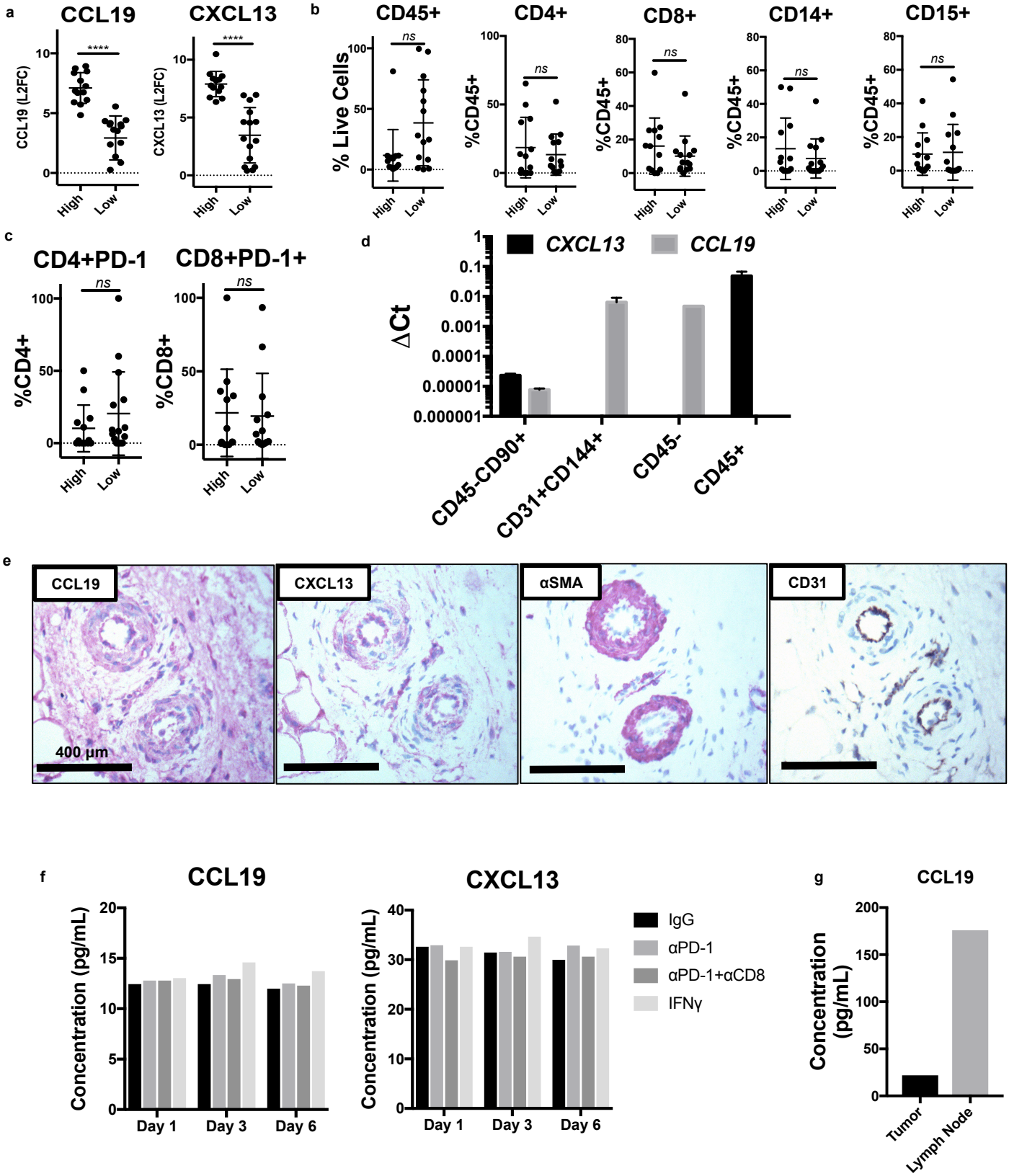

Supplementary Fig. 9

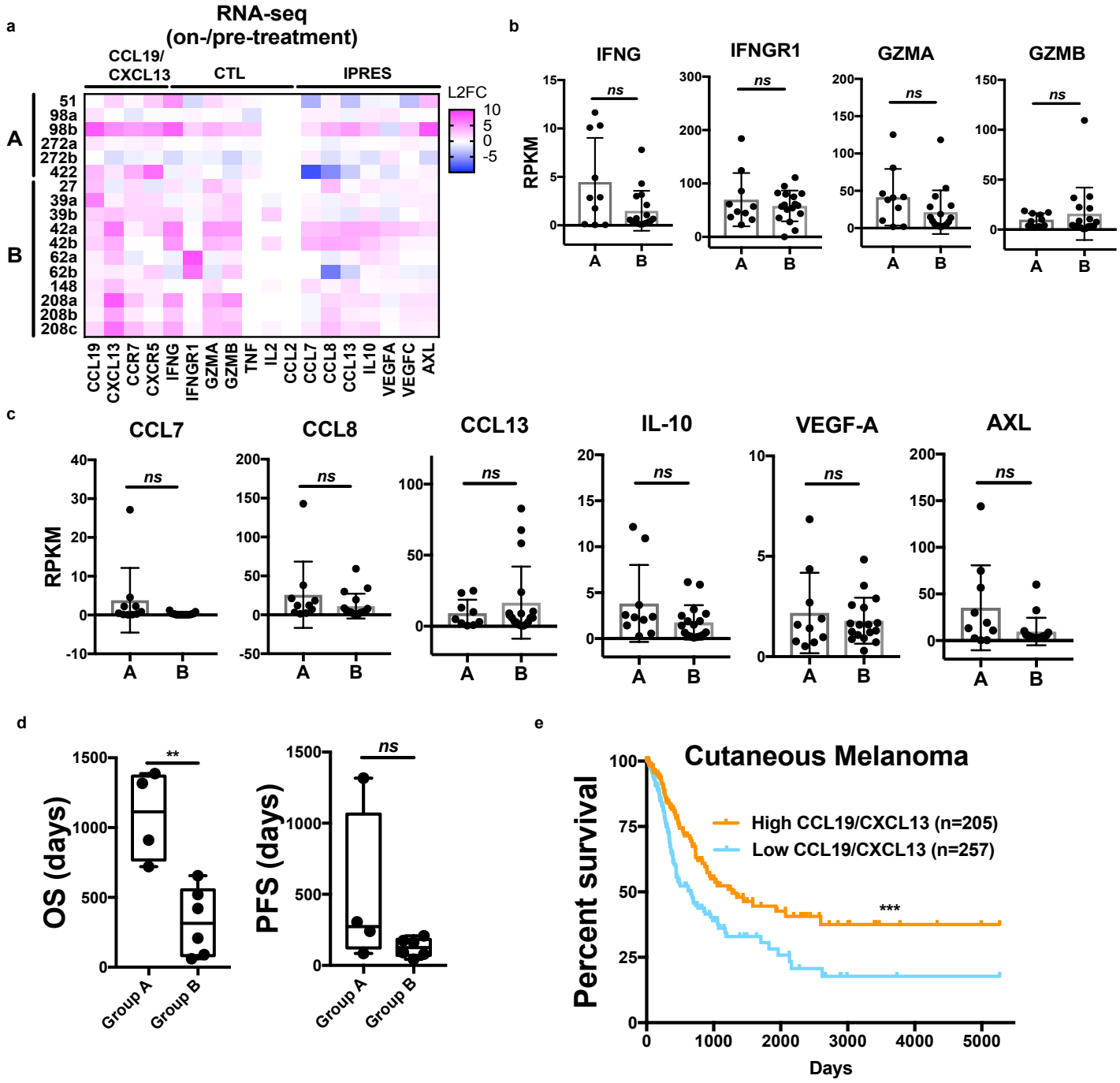

Supplementary Fig. 10